

Determination of the carrier envelope phase for short, circularly polarized laser pulses

Alexander I. Titov,¹ Burkhard Kämpfer,^{2,3} Atsushi Hosaka,^{4,5} Tobias Nusch,^{2,3} and Daniel Seipt^{6,7}

¹*Bogoliubov Laboratory of Theoretical Physics, Joint Institute for Nuclear Research, Dubna 141980, Moscow Region, Russia*

²*Helmholtz-Zentrum Dresden-Rossendorf, 01314 Dresden, Germany*

³*Institut für Theoretische Physik, TU Dresden, 01062 Dresden, Germany*

⁴*Research Center of Nuclear Physics, Osaka University, 10-1 Mihogaoka Ibaraki, 567-0047 Osaka, Japan*

⁵*J-PARC Branch, KEK, Tokai, Ibaraki, 319-1106, Japan*

⁶*Helmholtz-Institut Jena, Fröbelstieg 3, 07743 Jena, Germany*

⁷*Friedrich-Schiller-Universität Jena, Theoretisch-Physikalisches Institut, 07743 Jena, Germany*

(Received 18 December 2015; published 9 February 2016)

We analyze the impact of the carrier envelope phase on the differential cross sections of the Breit-Wheeler and the generalized Compton scattering in the interaction of a charged electron (positron) with an intensive ultrashort electromagnetic (laser) pulse. The differential cross sections as a function of the azimuthal angle of the outgoing electron have a clear bump structure, where the bump position coincides with the value of the carrier phase. This effect can be used for the carrier envelope phase determination.

DOI: [10.1103/PhysRevD.93.045010](https://doi.org/10.1103/PhysRevD.93.045010)

I. INTRODUCTION

The rapid progress in laser technology [1] offers novel and unprecedented opportunities to investigate quantum systems with intense laser beams [2]. A laser intensity I_L of $\sim 2 \times 10^{22}$ W/cm² has been already achieved [3]. Intensities of the order of $I_L \sim 10^{23} \dots 10^{25}$ W/cm² are envisaged in the near future, e.g. at CLF [4], ELI [5], or HiPER [6]. Further facilities are in the planning or construction stages, e.g. the PEARL laser facility [7] at Sarov/Nizhny Novgorod, Russia. The high intensities are provided in short pulses on a femtosecond pulse duration level [2,8,9], with only a few oscillations of the electromagnetic (e.m.) field or even subcycle pulses. (The tight connection of high intensity and short pulse duration is further emphasized in [10]. The attosecond regime will become accessible at shorter wavelengths [11,12].)

The new laser facilities utilize short and ultrashort pulses in “one-cycle” or “few-cycle” regimes. In this case, a determination of the pulse fine structure is very important and, in particular, tasking the phase difference between the electric field and pulse envelope, i.e. the carrier envelope phase (CEP). In the past, in the case of low beam intensity, the CEP determination has been achieved by averaging over a large number of phase-stabilized laser pulses. Later on, some methods for a determination of CEP were elaborated, for example, by studying above-threshold ion ionization [13,14], a direct measurement of the light waves of visible, ultraviolet, and/or infrared light using an electron attosecond probe [15]. As another possibility for CEP measurement it has been established to convert the light to the terahertz (THz) frequency range in a plasma, with subsequent analysis of the spatial charge asymmetry associated with THz emission [16].

However, such methods cannot be applied for high intensity laser pulses [17]. Therefore, another tool for the CEP determination for pulses with intensity $I \geq 10^{19}$ W/cm² needs to be developed. One avenue for getting access to the CEP is to search for observables which are both sensitive to the CEP variations and experimentally controllable. In Ref. [17], the effect of CEP is demonstrated in the angular distribution of the photons emitted by a relativistic electron via multiphoton Compton scattering off an intense linearly polarized short pulse. The asymmetries of azimuthal photon distributions in nonlinear Compton scattering were analyzed in [18]. The impact of the CEP on e^+e^- pair production with linearly polarized laser pulses is discussed in Ref. [19]. The importance of the CEP in Schwinger pair production in subcycle pulses is shown in [20]. Some other aspects of the effect of CEP in e^+e^- pair productions were discussed recently in [21–24].

Our present work may be considered as a further development of approaches to determine CEP for short and ultrashort *circularly polarized* laser pulses. We consider here both the generalized Breit-Wheeler process (e^+e^- pair production) and generalized Compton scattering (single photon emission off a relativistic electron). We limit our discussion to circularly polarized pulses: first, because the case of linear laser polarization has been already analyzed in [17,19,20]. And second, the methods elaborated in [25,26] for quantum processes with circularly polarized finite laser pulses (by utilizing the generalized Bessel functions) allow us to show the effect of the CEP on a transparent, almost qualitative level, which may be used as a powerful method for the CEP determination. Thus, we show that the azimuthal angle distributions of the emitted electron (positron) in the first case, and the recoil electron

(emitted photon) in the second case are in fact very sensitive to a CEP variation and can be used to fix the CEP value.

Our paper is organized as follows. In Sec. II we discuss the effect of the CEP in the case of the generalized Breit-Wheeler process. The impact of CEP on the generalized Compton scattering is analyzed in Sec. III. Our summary is given in Sec. IV.

II. EFFECT OF CEP IN BREIT-WHEELER e^+e^- PAIR PRODUCTION

A. The laser pulse

As we mentioned above, here we consider the generalized Breit-Wheeler process, i.e. the interaction of a probe photon X with a laser beam L in the reaction $X + L \rightarrow e^+ + e^-$, where a multitude of laser photons can participate simultaneously in the e^+e^- pair creation. The emphasis here is on short and intensive laser pulses. Long and weak laser pulses are dealt with in the standard textbook Breit-Wheeler process (cf. the review paper [27]). The different aspect of e^+e^- pair creation in finite pulses was also analyzed in Refs. [25,28–30]. Below, we will concentrate mainly on the effect of CEP, using the definitions of our Ref. [25].

In the following we use the widely employed e.m. four-potential for a circularly polarized laser field in the axial gauge $A^\mu = (0, \mathbf{A}(\phi))$ with

$$\mathbf{A}(\phi) = f(\phi)(\mathbf{a}_1 \cos(\phi + \tilde{\phi}) + \mathbf{a}_2 \sin(\phi + \tilde{\phi})), \quad (1)$$

where $\tilde{\phi}$ is the CEP. The quantity $\phi = k \cdot x$ is the invariant phase with four-wave vector $k = (\omega, \mathbf{k})$, obeying the null field property $k^2 = k \cdot k = 0$ (a dot between four-vectors indicates the Lorentz scalar product) implying $\omega = |\mathbf{k}|$, $\mathbf{a}_{(1,2)} \equiv \mathbf{a}_{(x,y)}$; $|\mathbf{a}_x|^2 = |\mathbf{a}_y|^2 = a^2$, $\mathbf{a}_x \mathbf{a}_y = 0$; and transversality means $\mathbf{k} \mathbf{a}_{x,y} = 0$ in the present gauge. The envelope function $f(\phi)$ with $\lim_{\phi \rightarrow \pm\infty} f(\phi) = 0$ accounts for the finite pulse duration. For simplicity and for the sake of numerical examples we use $f(\phi)$ in the form of a hyperbolic secant

$$f(\phi) = \frac{1}{\cosh \frac{\phi}{\Delta}}, \quad (2)$$

where the dimensionless quantity Δ is related to the pulse duration $2\Delta = 2\pi N$, where N has the meaning of a number of cycles in the pulse and it is related to the time duration of the pulse $\tau = 2N/\omega$. The carrier envelope phase $\tilde{\phi}$ is the main subject of our present discussion and, as we will show, its impact is particularly strong for short pulse duration Δ .

B. Cross section

The cross section of e^+e^- pair production is determined by the transition matrix $M_{fi}(\ell)$ as

$$\frac{d\sigma}{d\phi_e} = \frac{\alpha^2 v \zeta}{8m^4 \xi^2 N_0} \int_{\zeta}^{\infty} d\ell \int_{-1}^1 d\cos\theta_e |M_{fi}(\ell, u)|^2, \quad (E1)$$

$$(3)$$

where m is the electron mass, θ_e is the polar angle of outgoing electron, and v is the electron velocity in the c.m.s. In Eq. (3) the averaging and sum over the spin variables in the initial and the final states is assumed; the azimuthal angle of the outgoing electron ϕ_e is defined as $\cos\phi_e = \mathbf{a}_x \mathbf{p}_e / a |\mathbf{p}_e|$. The azimuthal angle of the positron momentum is $\phi_{e^+} = \phi_e + \pi$. The variable ξ is the reduced field intensity $\xi^2 = e^2 a^2 / m^2$. We use natural units with $c = \hbar = 1$, $e^2 / 4\pi = \alpha \approx 1/137.036$. The lower limit of the integral is the threshold parameter $\zeta = 4m^2/s$, where s is the square of the total energy in the c.m.s. The region of $\zeta < 1$ corresponds to the above-threshold e^+e^- pair production, while the region of $\zeta > 1$ matches the sub-threshold pair production. Denoting four-vectors $k(\omega, \mathbf{k})$, $k'(\omega', \mathbf{k}')$, $p(E, \mathbf{p})$ and $p'(E', \mathbf{p}')$ as the four-momenta of the background (laser) field (1), incoming probe photon, outgoing positron and electron, respectively, the variables s , v and u are determined as $s = 2k \cdot k' = 2(\omega'\omega - \mathbf{k}'\mathbf{k})$, $v^2 = (\ell s - 4m^2) / \ell s$, and $u \equiv (k' \cdot k)^2 / (4(k \cdot p)(k \cdot p')) = 1/(1 - v^2 \cos^2\theta_e)$. The factor N_0 reads $N_0 = 1/2\pi \int_{-\infty}^{\infty} d\phi (f^2(\phi) + f'^2(\phi))$ and determines the photon flux in the case of the finite pulse [26]. The variable ℓ saves continuous values and the product $\ell\omega$ has the meaning of the laser energy involved into the process (see also [21] for recent discussion).

The transition matrix $M_{fi}(\ell)$ in (3) consists of four terms

$$M_{fi}(\ell) = \sum_{i=0}^3 M^{(i)} C^{(i)}(\ell), \quad (4)$$

where the transition operators $M^{(i)}$ read

$$M^{(i)} = \bar{u}_{p'} \hat{M}^{BW(i)} v_p \quad (5)$$

with

$$\begin{aligned} \hat{M}^{BW(0)} &= \epsilon', \\ \hat{M}^{BW(1)} &= -\frac{e^2 a^2 (\epsilon' \cdot k) \mathbf{k}}{2(k \cdot p)(k \cdot p')}, \\ \hat{M}^{BW(2,3)} &= \frac{e a_{(1,2)} \mathbf{k} \epsilon'}{2(k \cdot p')} - \frac{e \epsilon' \mathbf{k} a_{(1,2)}}{2(k \cdot p)}, \end{aligned} \quad (6)$$

where $u_{p'}$ and v_p are the Dirac spinors of the electron and positron, respectively, and ϵ' is the polarization four-vector of the probe photon. The functions $C^i(\ell)$ can be written in terms of the basic functions Y_ℓ and X_ℓ which may be considered as the generalized Bessel functions for the finite e.m. pulse

$$\begin{aligned} Y_\ell(z) &= \frac{1}{2\pi} e^{-i\ell(\phi_0 - \tilde{\phi})} \int_{-\infty}^{\infty} d\phi f(\phi) e^{i\ell\phi - i\mathcal{P}(\phi)}, \\ X_\ell(z) &= \frac{1}{2\pi} e^{-i\ell(\phi_0 - \tilde{\phi})} \int_{-\infty}^{\infty} d\phi f^2(\phi) e^{i\ell\phi - i\mathcal{P}(\phi)} \end{aligned} \quad (7)$$

with

$$\begin{aligned} \mathcal{P}(\phi) &= z \int_{-\infty}^{\phi} d\phi' \cos(\phi' - \phi_0 + \tilde{\phi}) f(\phi') \\ &\quad - \xi^2 \zeta u \int_{-\infty}^{\phi} d\phi' f^2(\phi') \end{aligned} \quad (8)$$

in the following form,

$$\begin{aligned} C^{(0)}(\ell) &= \tilde{Y}_\ell(z) e^{i\ell(\phi_0 - \tilde{\phi})}, \\ \tilde{Y}_\ell(z) &= \frac{z}{2\ell} (Y_{\ell+1}(z) + Y_{\ell-1}(z)) - \xi^2 \frac{u}{u_\ell} X_\ell(z), \\ C^{(1)}(\ell) &= X_\ell(z) e^{i\ell(\phi_0 - \tilde{\phi})}, \\ C^{(2)}(\ell) &= \frac{1}{2} (Y_{\ell+1} e^{i(\ell+1)\phi_0} + Y_{\ell-1} e^{i(\ell-1)\phi_0}) e^{-i\ell\tilde{\phi}}, \\ C^{(3)}(\ell) &= \frac{1}{2i} (Y_{\ell+1} e^{i(\ell+1)\phi_0} - Y_{\ell-1} e^{i(\ell-1)\phi_0}) e^{-i\ell\tilde{\phi}}, \end{aligned} \quad (9)$$

where the argument z of the generalized Bessel functions is related to ξ , ℓ , and u via $z = 2\ell\xi\sqrt{u/u_\ell(1-u/u_\ell)}$ with $u_\ell \equiv \ell/\zeta$ and ϕ_0 is the azimuthal angle of outgoing electron $\phi_0 = \phi_e$. Equation (9) allows us to express the differential cross section in terms of the partial probabilities $w(\ell)$,

$$\frac{d\sigma}{d\phi_e} = \frac{\alpha^2 v \zeta}{4m^2 \xi^2 N_0} \int_{\zeta}^{\infty} d\ell \int_{-1}^1 d\cos\theta_e w(\ell) \quad (10)$$

with

$$\begin{aligned} w(\ell) &= 2|\tilde{Y}_\ell(z)|^2 + \xi^2(2u-1) \\ &\quad \times (|Y_{\ell-1}(z)|^2 + |Y_{\ell+1}(z)|^2 - 2\text{Re}(\tilde{Y}_\ell(z)X_\ell^*(z))), \end{aligned} \quad (11)$$

which resembles the known expression for the partial probability in the case of the infinitely long e.m. pulse [27]

$$w_n = 2J_n^2(z') + \xi^2(2u-1)(J_{n-1}^2(z') + J_{n+1}^2(z') - 2J_n^2(z'))$$

with the substitutions $\ell \rightarrow n$, $|\tilde{Y}_\ell(z)|^2 \rightarrow J_n^2(z')$, $|Y_{\ell\pm 1}(z)|^2 \rightarrow J_{n\pm 1}^2(z')$, $\text{Re}(\tilde{Y}_\ell(z)X_\ell^*(z)) \rightarrow J_n^2(z')$, and $z' = (2n\xi)/(1+\xi^2)^{1/2}\sqrt{u/u_n(1-u/u_n)}$ with $u_n \equiv n/\zeta$.

C. Numerical results

It is natural to expect that the effect of the finite carrier phase essentially appears in the azimuthal angle

distribution of the outgoing electron (positron) because the carrier phase is included in the expressions for the basic functions (7) in the combination $\phi_e - \tilde{\phi}$. As an example, in Fig. 1 (left panels) we show the differential cross section $d\sigma/d\phi_e$ of e^+e^- pair production as a function of the azimuthal angle ϕ_e for different values of the carrier envelope phase $\tilde{\phi}$ and for different pulse durations $\Delta = N\pi$ with $N = 0.5, 1, 1.5$ and 2 , and for $\xi^2 = 0.5$. The calculation is done for the essentially multiphoton region with $\zeta = 4$.

One can see a clear bumplike structure of the cross sections, in particular for very short pulses with $N \leq 1$, where the bump position coincides with the corresponding value of the carrier phase. In these cases the height of the bumps can reach orders of magnitude. The reason for such behavior is the following: The basic functions Y_ℓ and X_ℓ

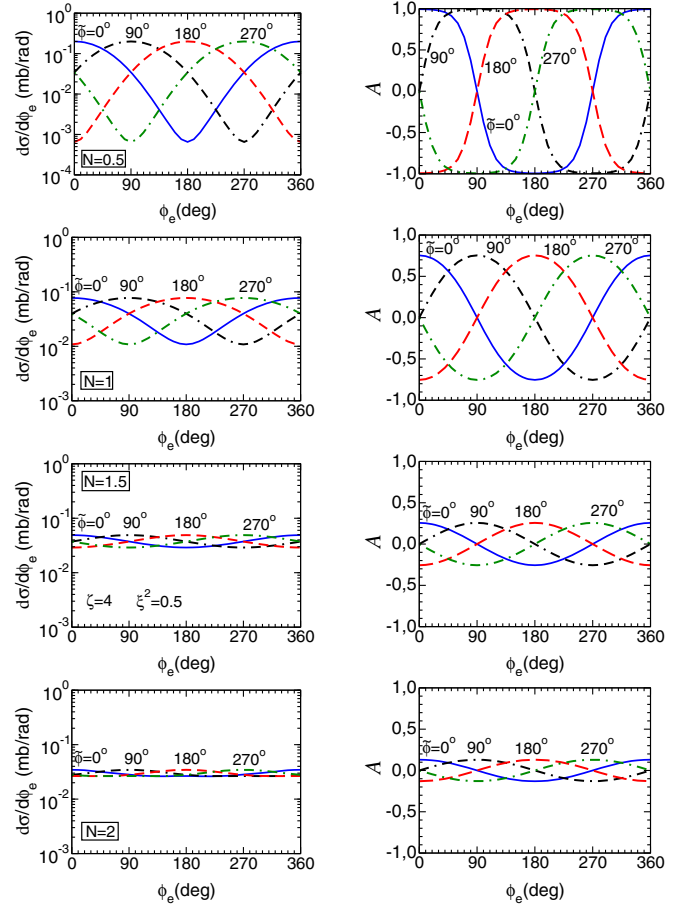


FIG. 1. Left column: The differential cross section as a function of the azimuthal angle of the direction of flight of the outgoing electron ϕ_e , for different values of the carrier phase $\tilde{\phi}$ and for different pulse duration $\Delta = N\pi$ with $N = 0.5, 1, 1.5$ and 2 (from the bottom panels). The solid, dash-dash-dotted, dashed and dash-dotted curves are for the CEP equal to $0^\circ, 90^\circ, 180^\circ$ and 270° degrees, respectively. Right column: The anisotropy (14) for different values of $\tilde{\phi}$ and N , as in the left column. $\xi^2 = 0.5$ and $\zeta = 4$.

are determined by the integral over $d\phi$ with a rapidly oscillating exponential function $\exp[i\Psi]$ with

$$\Psi = \ell\phi - z \left(\cos(\phi_e - \tilde{\phi}) \int_{-\infty}^{\phi} d\phi' f(\phi') \cos \phi' + \sin(\phi_e - \tilde{\phi}) \int_{-\infty}^{\phi} d\phi' f(\phi') \sin \phi' \right). \quad (12)$$

Then, taking into account the inequality for $\phi > 0$

$$\int_{-\infty}^{\phi} d\phi' f(\phi') \cos \phi' \gg \int_{-\infty}^{\phi} d\phi' f(\phi') \sin \phi', \quad (13)$$

which is valid for the smooth subcycle pulse shapes (e.g. for the hyperbolic secant shape), one can conclude that the main contribution to the probability comes from the region $\phi_e \approx \tilde{\phi}$, which is confirmed by the result of our full calculation shown in Fig. 1 (left panels). The effect of the carrier phase decreases with increasing pulse duration and for $N \geq 2$ it becomes negligibly small.

The corresponding anisotropies of the electron (positron) emission defined as

$$\mathcal{A} = \frac{d\sigma(\phi_e) - d\sigma(\phi_e + \pi)}{d\sigma(\phi_e) + d\sigma(\phi_e + \pi)}, \quad (14)$$

are exhibited in Fig. 1 (right panels). One can see a strong dependence of the anisotropy on CEP, especially for the subcycle pulses with $N = 0.5, 1$ which is a consequence of the ‘‘bump’’ structure of the differential cross sections shown in the left panels. In these cases the anisotropy takes a maximum value $\mathcal{A} \approx 1$ at $\phi_e = \tilde{\phi}$ and $|\mathcal{A}| < 1$ at $\phi_e \neq \tilde{\phi}$. It takes a minimum value $\mathcal{A} \approx -1$ at $\phi_e - \tilde{\phi} = \pm\pi$. The increase of the pulse duration leads to a decrease of the absolute value of \mathcal{A} .

Since the basic functions in (11) depend on the CEP through $\mathcal{P}(\phi)$ [cf. (8)] solely in combination $\phi_e - \tilde{\phi}$, then the cross sections and anisotropies depend on the scale variable $\Phi = \phi_e - \tilde{\phi}$. This means that the dependence of observables as a function of the rescaled azimuthal angle Φ are independent of the CE phase $\tilde{\phi}$ and they coincide with the dependence of these observables on ϕ_e at $\tilde{\phi} = 0$.

In Fig. 2 (left panel) we show the cross sections of e^+e^- pair production as a function of Φ for the subcycle pulse with $N = 0.5$ at different values of field intensity $\xi^2 = 0.1, 1, 10$. One can see that qualitatively the shape of the cross section is not sensitive to the value of ξ^2 . However the height of the bumps in the cross section slightly decreases with increasing ξ^2 .

Finally we note that the total cross section (integrated over ϕ_e) is not sensitive to the CEP. Thus, Fig. 2 (right panel) exhibits the total cross section of the e^+e^- pair production for the subcycle pulse with $N = 0.5$ and $\zeta = 4$ as a function of ξ^2 . The solid curve and crosses correspond

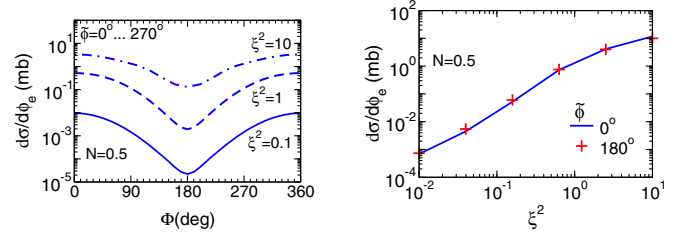


FIG. 2. Left panel: The cross section of the e^+e^- production as a function of scale variable $\Phi = \phi_e - \tilde{\phi}$ for different values of e.m. field intensities ξ . The solid, dashed and dash-dotted curves are for $\xi^2 = 0.1, 1, 10$, respectively. Right panel: The cross section of e^+e^- pair production integrated over ϕ_e as a function of ξ^2 for $\tilde{\phi} = 0$ (solid curve) and π (crosses). $N = 0.5$ and $\zeta = 4$.

to $\tilde{\phi} = 0$ and π , respectively. One can see in fact that the total cross section is independent of CEP.

III. IMPACT OF CEP ON THE GENERALIZED COMPTON SCATTERING

A. The cross section

The Compton scattering process, symbolically $e^- + L \rightarrow e^- + \gamma'$ is considered here as the spontaneous emission of one photon off an electron in an external e.m. field (1). Some important aspects of generalized Compton scattering were discussed elsewhere; see, for instance [18,31–36], and more recently [37]. Below we use the notations and definitions of Ref. [26].

We denote the four-momenta of the incoming electron, background (laser) field (1), outgoing electron and photon as $p(E, \mathbf{p})$, $k(\omega, \mathbf{k})$, $p'(E', \mathbf{p}')$, $k'(\omega', \mathbf{k}')$, respectively.

The cross section of the Compton scattering is determined by the transition matrix $M_{fi}(\ell)$ as

$$\frac{d\sigma}{d\omega' d\phi_{e'}} = \frac{\alpha^2}{N_0 \xi^2 (s - m^2) m^2} \int_{\delta\ell}^{\infty} d\ell \frac{|M_{fi}(\ell)|^2}{\|\mathbf{p}\| - \ell\omega}, \quad (15)$$

where the averaging and sum over the spin variable in the initial and the final states is assumed. The lower limit $\delta\ell$ may be smaller than 1 and, for instance, it may be determined by the detector resolution $\delta\omega'$ according to the relation among the frequency ω' of the emitted photon, auxiliary variable ℓ and the polar angle θ' of the direction of the momentum \mathbf{k}' thought the conservation laws as

$$\omega' = \frac{\ell\omega(E + |\mathbf{p}|)}{E + |\mathbf{p}| \cos \theta' + \ell\omega(1 - \cos \theta')}. \quad (16)$$

The frequency ω' increases with ℓ at fixed θ' since ω' is a function of ℓ at fixed θ' . All quantities are considered in the laboratory system.

Being a crossing channel to the Breit-Wheeler process, the main features of the Compton scattering formalism and the results are very close to those of the Breit-Wheeler

process, although there are some differences. Thus, there is no evident subthreshold effect because all frequencies ω' can contribute in (15) (see below, however, where we define specific subthreshold parameters responsible for the multiphoton effects).

The transition matrix $M(\ell)$ consists of four terms,

$$M(\ell) = \sum_{i=0}^3 M^{C(i)} C^{(i)}(\ell), \quad (17)$$

where the transition operators $M^{C(i)}$ are related to the transition operator $M^{BW(i)}$ in (6) as $M^{C(i)}(p, p', k, k') = M^{BW(i)}(-p, p', k, -k')$. The squared c.m.s. energy reads $s = m^2 + 2k \cdot p$. The coefficient functions $C^{(i)}(\ell)$ are determined by the basic functions according to Eqs. (9) but with their own phase function

$$\begin{aligned} \mathcal{P}(\phi) = & z \int_{-\infty}^{\phi} d\phi' \cos(\phi' - \phi_{e'} + \tilde{\phi}) f(\phi') \\ & - \xi^2 \frac{u}{u_1} \int_{-\infty}^{\phi} d\phi' f^2(\phi'), \end{aligned} \quad (18)$$

where the azimuthal angle of the recoil electron $\phi_{e'}$ coincides with the angle ϕ_0 in Ritus notation [27,38] and is determined as $\cos \phi_{e'} = \mathbf{a}_x \mathbf{p}' / a |\mathbf{p}'|$. The azimuthal angle of the photon momentum is $\phi_{\gamma'} = \phi_{e'} + \pi$. For the variables in Eq. (18) we use the standard notation: $z = 2\ell \xi ((u/u_{e'}) (1 - u/u_{e'}))^{1/2}$ with $u \equiv (k' \cdot k) / (k \cdot p')$, $u_{e'} = \ell u_1$ and $u_1 = (s - m^2) / m^2 = 2k \cdot p / m^2$. This representation of functions $C^{(i)}(\ell)$ allows us to define the differential cross section through the partial probabilities $w(\ell)$

$$\frac{d\sigma}{d\omega' d\phi_{e'}} = \frac{2\alpha^2}{N_0 \xi^2 (s - m^2)} \int_{\delta\ell}^{\infty} d\ell \frac{w(\ell)}{\|\mathbf{p}\| - \ell\omega} \quad (19)$$

with

$$\begin{aligned} w(\ell) = & -2|\tilde{Y}_{\ell}(z)| + \xi^2 \left(1 + \frac{u^2}{2(1+u)} \right) \\ & \times (|Y_{\ell-1}(z)|^2 + |Y_{\ell+1}(z)|^2 - 2\text{Re}(\tilde{Y}_{\ell}(z) X_{\ell}^*(z))). \end{aligned} \quad (20)$$

Equation (20) resembles the corresponding expression for the partial probability of photon emission in the case of the infinitely long pulse [27,38] with the substitutions $\ell \rightarrow n$, $|\tilde{Y}_{\ell}(z)|^2 \rightarrow J_n^2(z')$, $|Y_{\ell\pm 1}(z)|^2 \rightarrow J_{n\pm 1}^2(z')$, and $\text{Re}(\tilde{Y}_{\ell}(z) X_{\ell}^*(z)) \rightarrow J_n^2(z')$,

$$\begin{aligned} w_n = & -2J_n^2(z') + \xi^2 \left(1 + \frac{u^2}{2(1+u)} \right) \\ & \times (J_{n-1}^2(z') + J_{n+1}^2(z') - 2J_n^2(z')), \end{aligned}$$

where $J_n(z')$ denotes Bessel functions with $z' = 2n\xi / (1 + \xi^2)^{1/2} (u/u_n (1 - u/u_n))^{1/2}$ and $u_n = (2n(k \cdot p)) / (m^2 (1 + \xi^2))$.

We recall that the internal quantity ℓ is a continuous variable, implying a continuous distribution of the differential cross section over the $\omega' - \theta'$ plane. The case of $\ell = 1$ with $\xi^2 \ll 1$ and $\omega'_1 = \omega'(\ell = 1)$ recovers the Klein-Nishina cross section, cf. [27]. The quantity $\ell\omega$ can be considered as an energy of the laser beam involved in the Compton process, which is not a multiple ω . Mindful of this fact, without loss of generality, we denote the processes with $\ell > 1$ as a multiphoton generalized Compton scattering, remembering that ℓ is a continuous quantity. We stress again, the internal variable ℓ cannot be interpreted strictly as the number of laser photons involved (cf. [39]).

The cross section of the multiphoton Compton scattering (for $\ell > 1$) first increases with increasing θ' and peaks at a scattering angle $\theta' < 180^\circ$, beyond which it rapidly drops to zero when θ' approaches 180° , yielding the blind spot in the high harmonics for back-scattering. For instance, the cross section peaks at about 170° for the chosen electron energy of 4 MeV (all quantities are considered in the laboratory frame).

Therefore, in our subsequent analysis we choose the near-backward photon production at $\theta' = 170^\circ$ and an optical laser with $\omega = 1.55$ eV. Defining one-photon events by $\ell = n = 1$, this kinematics leads via Eq. (16) to $\omega'_1 \equiv \omega'(l = 1, \theta' = 170^\circ) \approx 0.133$ keV which we refer to as a threshold value. Accordingly, $\omega' > \omega'_1$ is enabled by nonlinear effects which in turn may be related loosely to multiphoton dynamics.

The ratio $\kappa = \omega' / \omega'_1$ may be considered as a subthreshold parameter (as an analog of subthreshold parameter ζ in the Breit-Wheeler process). Using the value $\kappa \approx \ell'(\omega'(\ell'))$ we can define the subthreshold part of the total cross section $\tilde{\sigma}$ explicitly as the integral

$$\frac{\tilde{\sigma}(\omega')}{d\phi_{e'}} = \int_{\omega'}^{\infty} d\bar{\omega} \frac{d\sigma(\bar{\omega})}{d\bar{\omega} d\phi_{e'}} = \int_{\ell'(\kappa)}^{\infty} d\ell \frac{d\sigma(\ell)}{d\ell d\phi_{e'}}, \quad (21)$$

where $d\sigma(\ell) / d\ell d\phi_{e'} = (d\sigma(\omega') / d\omega' d\phi_{e'}) (d\omega'(\ell) / d\ell)$, and the minimum value of $\ell'(\kappa)$ is

$$\ell'(\kappa) = \kappa \frac{E + |\mathbf{p}| \cos \theta'}{E + |\mathbf{p}| \cos \theta' - \omega(\kappa - 1)(1 - \cos \theta')}. \quad (22)$$

The cross section (21) has the meaning of a cumulative distribution. In this case, the subthreshold, multiphoton events correspond to frequencies ω' of the outgoing photon which exceed the corresponding threshold value $\omega'_1 = \omega'(\ell = 1)$ [cf. Eq. (16)].

Similarly to the Breit-Wheeler process, the effect of the finite CEP essentially appears in the differential cross sections as a function of the azimuthal angle of the outgoing electron (photon) momentum because the carrier

phase is included in the expressions for the basic functions (7) with (18) in combination $\phi_{e'} - \tilde{\phi}$.

B. Numerical results

The differential cross section (19) as a function of the azimuthal angle $\phi_{e'}$ for different values of the carrier phase $\tilde{\phi}$ for the pulses with $N = 0.5, 1, 1.5$ and 2 for the hyperbolic secant shape with $\kappa = \omega'/\omega'_1 = 3$ and $\xi^2 = 0.5$ is exhibited in the left panels of Fig. 3.

One can see a clear bumplike structure of the distribution, where the bump position coincides with the corresponding value of the carrier phase. The reason for such behavior is the same as in the case of the Breit-Wheeler process, explained by the highly oscillating factor in Eq. (12) with inequality (13) valid for very short pulses.

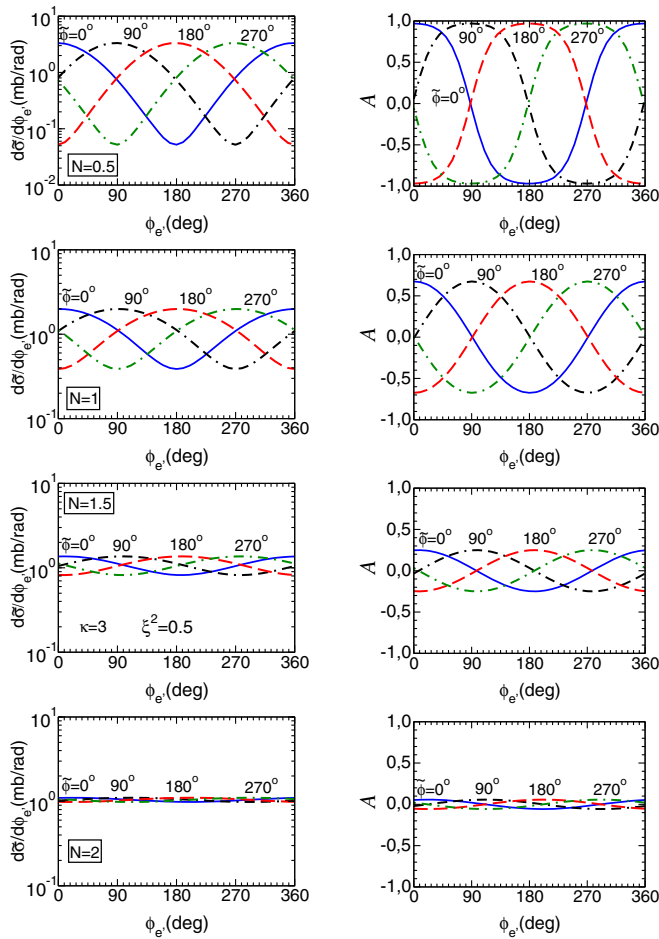


FIG. 3. Left column: The differential cross section (19) as a function of the azimuthal angle of the outgoing electron momentum $\phi_{e'}$ for different values of the carrier phase $\tilde{\phi}$ and different numbers of cycles in a pulse, N , as depicted in the plots. The solid, dash-dash-dotted, dashed and dash-dotted curves correspond to the carrier phases equal to $0, 90, 180$ and 270 degrees, respectively. Right column: The anisotropy as a function of $\phi_{e'}$ for different $\tilde{\phi}$, for the hyperbolic secant shape with $N = 0.5$. $\xi^2 = 0.5$ and $\kappa = \omega'/\omega'_1 = 3$.

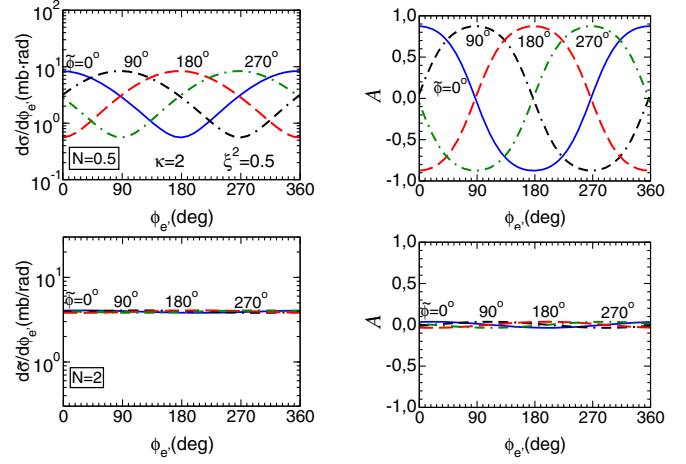


FIG. 4. The same as in Fig. 3 but for $\kappa = 2$ and for two values of $N = 0.5$ (top row) and 2 (bottom row).

The impact of CEP decreases with increasing pulse duration (or N) and becomes very small at $N > 2$ which is in agreement with the prediction of [17] for the linearly polarized pulse.

Corresponding anisotropies defined by Eq. (14) with substitution $d\sigma(\phi_e) \rightarrow d\sigma(\phi_{e'})$ are exhibited in the right panels of Fig. 3. One can see a strong dependence of the anisotropy on the carrier phase for the short pulses which resembles the pattern of the differential cross sections shown in the left panels. The maximum effect is expected for the subcycle pulse with $N = 0.5$, where similar to the Breit-Wheeler process, the anisotropy takes a maximum value $\mathcal{A} \approx 1$ at $\phi_{e'} = \tilde{\phi}$ and $|\mathcal{A}| < 1$ at $\phi_{e'} \neq \tilde{\phi}$. It takes a minimum value $\mathcal{A} \approx -1$ at $\phi_{e'} - \tilde{\phi} = \pm\pi$. For the short pulses with $N = 2$ the absolute value of the anisotropy is much lower than 1.

The CEP effect is sensitive to the subthreshold parameter $\kappa = \omega'/\omega'_1$. Our prediction for $\kappa = 2$ is exhibited in Fig. 4.

In this case the effect of CEP is smaller. Thus, for $N = 0.5$ the heights of the bumps in the cross sections decrease by more than a factor of four compared to the case of $\kappa = 3$. The impact of CEP practically disappears for $N \geq 2$.

Finally we note that similarly to the Breit-Wheeler process, the differential cross sections and anisotropies of the generalized Compton process are the functions of the scale variable $\Phi = \phi_{e'} - \tilde{\phi}$ which leads to independence of the corresponding observables from $\tilde{\phi}$ (at fixed Φ), and independence of cross sections integrated over $\phi_{e'}$ from CEP, similarly to the results presented in Fig. 2.

IV. SUMMARY

In summary we have considered the carrier envelope phase (CEP) effect in a short circularly polarized electromagnetic (laser) pulse for e^+e^- pair production (generalized Breit-Wheeler process) and for emission of a single photon off of a relativistic electron (generalized Compton

scattering) produced in an essentially multiphoton region. In both cases we found a strong dependence of the differential cross sections as a function of the azimuthal angle of the outgoing particle on CEP. In the first case it is the azimuthal angle of the outgoing electron (positron), while in the second case it is the azimuthal angle of the recoil electron (or photon). For very short pulses the corresponding cross sections have a bumplike structure where the bump position coincides with the CEP value. The heights of the bumps for subcycle pulses with $N \leq 1$ reach orders of magnitude. This means that studying the azimuthal angle distributions may be used as a unique and

powerful method for the CEP determination in the case of a circularly polarized laser beam. The CEP effect decreases quite clearly with increasing pulse duration and becomes negligible for pulses with number of oscillations $N \geq 3$. Note that this effect becomes relevant in the essentially multiphoton (cumulative) region.

ACKNOWLEDGMENTS

The authors acknowledge fruitful discussions with R. Sauerbrey and T.E. Cowan within the Helmholtz International Beamline Extreme Field project [40].

-
- [1] G. A. Mourou, T. Tajima, and S. V. Bulanov, Optics in the relativistic regime, *Rev. Mod. Phys.* **78**, 309 (2006).
- [2] A. Di Piazza, C. Müller, K. Z. Hatsagortsyan, and C. H. Keitel, Extremely high-intensity laser interactions with fundamental quantum systems, *Rev. Mod. Phys.* **84**, 1177 (2012).
- [3] V. Yanovsky *et al.*, Ultra-high intensity 300-TW laser at 0.1 Hz repetition rate, *Opt. Express* **16**, 2109 (2008).
- [4] Central Laser Facility (CLF), <http://www.clf.stfc.ac.uk/CLF/>.
- [5] Extreme Light Infrastructure - European Project (ELI), <http://www.eli-beams.eu>.
- [6] European High Power Laser Energy Research (HIPER), <http://www.hiper-laser.org>.
- [7] Laser Project of the Institute of Applied Physics, Russian Acad. Sci., http://www.ipfran.ru/english/science_e.html.
- [8] A. L. Cavalieri *et al.*, Intense 1.5-cycle near infrared laser waveforms and their use for the generation of ultra-broadband soft-x-ray harmonic continua, *New J. Phys.* **9**, 242 (2007).
- [9] Z. Major, S. Klingebiel, C. Skrobol, I. Ahmad, C. Wandt, S. A. Trushin, F. Krausz, S. Karsch, and D. Dumitras, Status of the Petawatt Field Synthesizer pumpseed synchronization measurements, *AIP Conf. Proc.* **1228**, 117 (2010).
- [10] F. Mackenroth and A. Di Piazza, Nonlinear Compton scattering in ultra-short laser pulses, *Phys. Rev. A* **83**, 032106 (2011).
- [11] X. Feng, S. Gilbertson, H. Mashiko, He Wang, S. D. Khan, M. Chini, Yi Wu, K. Zhao, and Z. Chang, Generation of Isolated Attosecond Pulses with 20 to 28 Femtosecond Lasers, *Phys. Rev. Lett.* **103**, 183901 (2009).
- [12] F. Krausz and M. Ivanov, Attosecond physics, *Rev. Mod. Phys.* **81**, 163 (2009).
- [13] G. G. Paulus, F. Lindner, H. Walther, A. Baltuška, E. Goulielmakis, M. Lezius, and F. Krausz, Measurement of the Phase of Few-Cycle Laser Pulses, *Phys. Rev. Lett.* **91**, 253004 (2003).
- [14] T. Wittmann, B. Horvath, W. Helml, M. G. Schätzel, X. Gu, A. L. Cavalieri, G. G. Paulus, and R. Kienberger, Single-shot carrier-envelope phase measurement of few-cycle laser pulses, *Nat. Phys.* **5**, 357 (2009).
- [15] E. Goulielmakis *et al.*, Direct measurement of light waves, *Science* **305**, 1267 (2004).
- [16] M. Kieß *et al.*, Determination of the carrier-envelope phase of few-cycle laser pulses with terahertz-emission spectroscopy, *Nat. Phys.* **2**, 327 (2006).
- [17] F. Mackenroth, A. Di Piazza, and C. H. Keitel, Determining the Carrier-Envelope Phase of Intense Few-Cycle Laser Pulses, *Phys. Rev. Lett.* **105**, 063903 (2010).
- [18] D. Seipt and B. Kämpfer, Asymmetries of azimuthal photon distributions in non-linear Compton scattering in ultra-short intense laser pulses, *Phys. Rev. A* **88**, 012127 (2013).
- [19] K. Krajewska and J. Z. Kaminski, Breit-Wheeler process in intense short laser pulses, *Phys. Rev. A* **86**, 052104 (2012).
- [20] F. Hebenstreit, R. Alkofer, G. V. Dunne, and H. Gies, Momentum Signatures for Schwinger Pair Production in Short Laser Pulses with a Subcycle Structure, *Phys. Rev. Lett.* **102**, 150404 (2009).
- [21] M. J. A. Jansen and C. Müller, Strong-field Breit-Wheeler pair production in short laser pulses: Identifying multiphoton interference and carrier-envelope phase effects, [arXiv:1511.07660](https://arxiv.org/abs/1511.07660).
- [22] A. Nuriman, Zi-Liang Li, and Bai-Song Xie, Effects of laser pulse shape and carrier envelope phase on pair production, *Phys. Lett. B* **726**, 820 (2013).
- [23] S. Meuren, C. H. Keitel, and A. Di Piazza, Semiclassical picture for electron-positron photoproduction in strong laser fields, [arXiv:1503.03271](https://arxiv.org/abs/1503.03271).
- [24] S. Meuren, K. Z. Hatsagortsyan, C. H. Keitel, and A. Di Piazza, Polarization-operator approach to pair creation in short laser pulses, *Phys. Rev. D* **91**, 013009 (2015).
- [25] A. I. Titov, B. Kämpfer, H. Takabe, and A. Hosaka, Breit-Wheeler process in very short electromagnetic pulses, *Phys. Rev. A* **87**, 042106 (2013).
- [26] A. I. Titov, B. Kämpfer, T. Shibata, A. Hosaka, and H. Takabe, Laser pulse-shape dependence of Compton scattering, *Eur. Phys. J. D* **68**, 299 (2014).
- [27] V. I. Ritus, *Akad. Nauk SSSR* **111**, 5 (1979) [*J. Sov. Laser Res. (United States)* **6**:5, 497 (1985)].
- [28] A. I. Titov, H. Takabe, B. Kämpfer, and A. Hosaka, Enhanced Subthreshold Electron-Positron Production in Short Laser Pulses, *Phys. Rev. Lett.* **108**, 240406 (2012).

- [29] T. Nousch, D. Seipt, B. Kämpfer, and A. I. Titov, Pair production in short laser pulses near threshold, *Phys. Lett. B* **715**, 246 (2012).
- [30] K. Krajewska and J. Z. Kaminski, Breit-Wheeler process in intense short laser pulses, *Phys. Rev. A* **86**, 052104 (2012).
- [31] M. Boca and V. Florescu, Nonlinear Compton scattering with a laser pulse, *Phys. Rev. A* **80**, 053403 (2009).
- [32] T. Heinzl, D. Seipt, and B. Kämpfer, Beam-shape effects in nonlinear Compton and Thomson scattering, *Phys. Rev. A* **81**, 022125 (2010).
- [33] D. Seipt and B. Kämpfer, Non-linear Compton scattering of ultrashort and ultraintense laser pulses, *Phys. Rev. A* **83**, 022101 (2011).
- [34] V. Dinu, T. Heinzl, and A. Ilderton, Infra-red divergences in plane wave backgrounds, *Phys. Rev. D* **86**, 085037 (2012).
- [35] D. Seipt and B. Kämpfer, Two-photon Compton process in pulsed intense laser fields, *Phys. Rev. D* **85**, 101701 (2012).
- [36] K. Krajewska and J. Z. Kaminski, Compton process in intense short laser pulses, *Phys. Rev. A* **85**, 062102 (2012).
- [37] K. Krajewska, F. Cajiao Vlez, and J. Z. Kaminski, Generalized Klein-Nishina formula, *Phys. Rev. A* **91**, 062106 (2015).
- [38] V. B. Berestetskii, E. M. Lifshitz, and L. P. Pitaevskii, *Quantum Electrodynamics*, Course of Theoretical Physics, 2nd ed., Vol. 4 (Pergamon Press, Oxford, New York, 1982).
- [39] D. Seipt and B. Kämpfer, Laser-assisted Compton scattering of x-ray photons, *Phys. Rev. A* **89**, 023433 (2014).
- [40] Helmholtz International Beamline for External Fields, <http://www.hzdr.de/db/Cms?pOid=35325&pNid=3214>.